Journal of
*Marine Science and Engineering*

MDPI

*Article*

# Effect of UV and Visible Radiation on Optical Properties of Chromophoric Dissolved Organic Matter Released by *Emiliania huxleyi*

**Simona Retelletti Brogi [1], Bruno Charrière [2], Margherita Gonnelli [1], Frédéric Vaultier [3], Richard Sempéré [3], Stefano Vestri [1] and Chiara Santinelli [1,*]**

[1] CNR—Institute of Biophysics, 56124 Pisa, Italy; simona.retelletti@ibf.cnr.it (S.R.B.); margherita.gonnelli@pi.ibf.cnr.it (M.G.); vestri@pi.ibf.cnr.it (S.V.)
[2] CEFREM, Université de Perpignan, CNRS UMR 5110, 66860 Perpignan, France; bruno.charriere@univ-perp.fr
[3] Mediterranean Institute of Oceanography (M I O) UM 110, Aix Marseille University, Universite de Toulon, CNRS, IRD, 13288 Marseille, France; frederic.vaultier@mio.osupytheas.fr (F.V.); richard.sempere@mio.osupytheas.fr (R.S.)
* Correspondence: chiara.santinelli@ibf.cnr.it; Tel.: +39-050-3152755

Received: 30 September 2020; Accepted: 5 November 2020; Published: 7 November 2020

check for updates

**Abstract:** Photodegradation is a natural process that strongly affects the chromophoric fraction of dissolved organic matter (DOM), especially in surface water of the oceans. In the euphotic zone, the concentration and quality of DOM are mostly dependent on primary production by phytoplankton. The effect of photodegradation on algal DOM has not been investigated as much as on terrestrial DOM. In this study, we explored the effect of different spectral regions (i.e., full sun spectrum, visible light, 295–800 nm, 305–800 nm, and 320–800 nm) on algal exudates by *Emiliania huxleyi*, a ubiquitous coccolithophore. The optical properties (absorption and fluorescence) of algal DOM were investigated before and after irradiation with the different spectral regions. The absorption and fluorescence spectra were compared before and after irradiation. The results showed an increase in the effect of photobleaching with increasing irradiation energy for all of the absorbance indices. Similarly, the protein-like fluorescence decreased at increasing irradiation energy. The humic-like fluorescence, which was the most affected, did not show a linear trend between photobleaching and irradiation energy, which suggested that irradiation mainly determined a change in these molecules' quantum yield.

**Keywords:** chromophoric dissolved organic matter; photobleaching; phosphorescence; fluorescence; *Emiliania huxleyi*

## 1. Introduction

Dissolved organic matter (DOM) is a complex mixture of organic molecules representing one of Earth's largest exchangeable carbon reservoirs. DOM is actively involved in the marine food web as a source of energy for heterotrophic prokaryotes and as byproducts of biological metabolism [1]. Primary production in the ocean's euphotic zone sets the upper limit of DOM production in the marine environment, even though other processes can contribute to its release. A combination of phytoplankton community structure and environmental conditions can determine the release of organic compounds from these autotrophic organisms ([1] and references therein).

Once in the marine environment, DOM undergoes several processes that can lead to its removal and/or transformation. In surface waters, photochemical processes are one of the major pathways of transformation and the removal of DOM in the aquatic environment [2]. The chromophoric DOM

(CDOM) is the fraction of DOM that absorbs light at the UV and visible wavelengths; it is therefore the fraction most affected by photochemical processes. A fraction of CDOM can also emit a part of the absorbed light as fluorescence. When DOM is exposed to the light it can be photomineralized, leading to an input of CO, $CO_2$, and other volatile compounds to the atmosphere [3–5], it can be photobleached, with the transformation of CDOM in smaller and less absorbing molecules favoring bacterial growth [3,6,7], or it can undergo photohumification leading to a reduction of DOC bioavailability [8]. In the global ocean, CDOM is responsible for nearly 90% of ultraviolet (UV) radiation attenuation [9]; therefore, its reduction can lead to (1) a reduction of its protecting function against DNA damages on marine organisms [10] and (2) a deeper penetration of a larger amount of UV radiation, also affecting primary production. It has been shown that photobleaching can produce labile compounds, such as low molecular weight organic compounds, phosphorus, and nitrate-rich compounds, which can stimulate the biological activity [11]. Conversely, photohumification processes can reduce DOM bioavailability [8,12,13].

Several studies focused on the effect of irradiation on DOM removal and/or on changes in CDOM properties [3,14–20], as well as on the changes in its bioavailability [8,11–22]. However, most of these studies concern the irradiation of terrestrial DOM, mostly in rivers, lakes, and coastal areas, whereas information on the effects of irradiation on DOM that is released by phytoplankton are limited [22–25].

In this framework, irradiation experiments were carried out on algal exudates from *Emiliania huxleyi*, in order to obtain new insights into the quantitative and qualitative changes on algal DOM that is induced by UV and Visible radiations.

*Emiliania huxleyi* was selected, since it is the most abundant species of coccolithophores in the world's oceans [26] and the coccolithophores represent one of the major phytoplankton group [27] and can be found globally [28]. Therefore, it can be a good model for primary producers of autochthonous DOM in the ocean. To study the effects of irradiation on the DOM released by *E. huxleyi*, changes in its optical properties (absorption and fluorescence) as well as in DOC concentration were evaluated.

## 2. Materials and Methods

### 2.1. *Emiliania huxleyi* Culture and Samples Preparation

*Emiliania huxleyi* strain RCC1215 obtained from the Roscoff Culture Collection of Living Microalgae were maintained at 20 °C in 50 mL glass Erlenmeyer flasks in f/2 medium [29] and 36 Joules $m^2$ $s^{-1}$. A volume of 375 mL of the culture was used to inoculate 6 L of f/2 medium aerated in a 10 L Nalgene autoclavable polycarbonate carboy. The culture was then grown at 17 °C in a constant environment-controlled cabinet under 36 Joules $m^{-2}$ $s^{-1}$ (Photosynthetically Acrive Radiation, PAR) of cool-white fluorescent light with a 12:12 h light:dark (LD) cycle. The cultures were gently hand-shaken regularly, and the algal exudates were collected at the beginning of the stationary phase, after 16 days. The stationary phase was determined to be the time between the end of the log-linear portion of the growth curve and until the end of the growth curve. In order to obtain the algal exudates the culture was filtered in dim light through pre-combusted 0.7 µm glass fiber (GF/F) filters, which had been pre-rinsed with seawater. The samples were then filtered through 0.2 µm Nuclepore polycarbonate filters, previously rinsed with 10% HCl solution, Milli-Q water, and finally with the sample.

### 2.2. Irradiation Experiment

The samples were irradiated for 10 h using a Suntest Atlas CPS+ solar simulator 750 W (Atlas Material Testing Technology, Illinois, IL, USA), with different spectral regions selected using long-band-pass cutoff filters (Schott models):

- WG280: 280–800 nm, representing the full sun spectrum (hereinafter FS).
- WG295: 295–800 nm (hereinafter $I_{295–800}$).
- WG305: 305–800 nm (hereinafter $I_{305–800}$).
- WG320: 320–800 nm (hereinafter $I_{320–800}$).

- WG395: 395–800 nm, representing the visible radiation (hereinafter Vis).

Over the 10 h irradiation, PAR (400–800 nm), UV-A (280–315 nm), and UV-B (400–800 nm) doses were 24,000, 3000, and 123 Kj m$^2$, respectively. These doses correspond to 3–4 days of natural irradiation measured using a broadband filter radiometer (ELDONET, Real Time Computers, Inc., Germany, data not shown) at Marseille in spring, during *Emiliania huxleyi* bloom.

Note that full sun spectrum irradiation (FS) does not replicate natural conditions since the solar radiations between 280 and 295 nm do not reach the Earth's surface [30].

Each irradiation treatment was carried out in duplicate due to the limited amount of exudates that were obtained from the culture.

### 2.3. Dissolved Organic Carbon (DOC) Measurements

DOC measurements were carried out by high-temperature catalytic oxidation while using a Shimadzu TOC- VCSN (Shimadzu Corporation, Kyoto, Japan) following the method that was reported by Santinelli et al. [31]. The reliability of measurements was controlled twice a day by comparison of data with a DOC reference seawater sample [32] (CRM Batch #12 nominal concentration of 41–44 µM; measured concentration 43.7 µM).

### 2.4. CDOM Absorbance

CDOM absorbance was measured throughout the UV and visible spectral domains (230–700 nm) using a spectrophotometer (JASCO, V-550, Jasco company, Tokyo, Japan) and a 10 cm quartz cell. The medium used for the E. huxleyi culture was subtracted as a blank for each spectrum, in order to remove the signal of the original water. The absorption parameters were calculated using the ASFit software [33]. The absorption coefficients were calculated at 254 nm ($a_{254}$) and 350 nm ($a_{350}$), while using the following equation.

$$a_\lambda = 2.303\,\frac{A_\lambda - A_{650\text{–}700}}{l} \quad (1)$$

where $A_\lambda$ is the absorbance at wavelength λ, $A_{650\text{–}700}$ is the average absorbance between 650 and 700 nm, and l is the cuvette path length (i.e., 0.1 m). The average absorbance between 650 and 700 nm was subtracted from each spectrum to remove residual scattering, or changes not ascribable to organic matter [34]. The molecular size (MS; i.e., the mean molecular weight) of CDOM was calculated as the ratio $a_{250}/a_{365}$ [35,36]. The specific ultraviolet absorption ($SUVA_{254}$) was calculated as the ratio between the decadic absorption at 254 nm ($A_{254}/L$) and DOC concentration [37], and it was reported as $m^2\ g^{-1}C$. The spectral slope was calculated in the 275–295 nm range ($S_{275\text{–}295}$), and in the 350–400 nm ($S_{350\text{–}400}$) in order to calculate Sr ($S_{275\text{–}295}/S_{350\text{–}400}$) [35], using the following equation

$$a_\lambda = a_{\lambda_0} \cdot e^{-S(\lambda-\lambda_0)} \quad (2)$$

### 2.5. Fluorescence Emission Spectra

Fluorescence emission spectra were measured by a FluoroMax4 spectrofluorometer model FP770 (Horiba Ltd., Kyoto, Japan). Three excitation wavelengths were used.

- 280 nm, to study the protein-like DOM fluorescence (emission was recorded between 290 and 500 nm) [38,39];
- 290 nm, because it is selective for tryptophan residues (emission was recorded between 300 and 500 nm) [40]; and,
- 355 nm, to study the humic-like DOM fluorescence (emission was recorded between 365 and 600 nm) [38,39].

The medium used for the E. huxleyi culture was subtracted as a blank from each spectrum. Each fluorescence spectrum was corrected for instrument bias in excitation and emission and inner-filtering effect [40]. The fluorescence intensity was normalized by the integrated area under a Milli-Q water Raman peak (λex = 350 nm, λem = 371–428 nm, [41]) measured the same day of the analysis; the fluorescence data are reported as Raman Unit (R.U.).

### 2.6. Fluorescence EEMs

The tridimensional Excitation-Emission matrixes (EEMs) were recorded while using the Aqualog spectrofluorometer (Horiba Ltd, Kyoto, Japan). This instrument uses a charge-coupled device (CCD) to reveal the signal, guaranteeing a high acquisition velocity and reduced photobleaching. The excitation (Ex) wavelength ranged between 250 and 450 nm at 5 nm increment, while emission (Em) was measured between 212 and 619 nm at 3 nm increments. EEMs were corrected for instrument bias in excitation and emission and inner-filtering effect [40]. EEMs were subtracted by the blank (i.e., the medium used for the E. huxleyi culture). The Rayleigh and Raman scatter peaks were removed while using the monotone cubic interpolation (shape-preserving) [42]. The fluorescence intensity was normalized by the integrated area under a Milli-Q water Raman peak (λex = 350 nm, λem = 371–428 nm, [41]) that was measured the same day of the analysis; data are reported as Raman Unit (R.U.). The EEMs were elaborated using the TreatEEM software (Omanovic Dario, TreatEEM—program for treatment of fluorescence excitation-emission matrices, https://sites.google.com/site/daromasoft/home/treateem). The DOM typical peaks were identified according to Coble [43]: Peak A, Ex/Em = 260/380–460; Peak C, Ex/Em = 350/420–480; Peak M, Ex/Em = 310/380–420; Peak T, Ex/Em = 275/340; Peak B, Ex/Em = 275/310.

## 3. Results

### 3.1. DOC Concentration

The DOC concentration was 1190 ± 6 µM in the non-irradiated samples. A small decrease, i.e., 10–16%, was observed in the samples that were irradiated using the 295, 305, and 320 nm cutoff filters, whereas the FS irradiated samples only showed a 3% decrease. The data of the Vis-irradiated samples are unfortunately not available due to a technical problem during DOC analysis.

### 3.2. CDOM Absorption

The absorption spectra of CDOM (before and after irradiation with different wavelengths) showed the classical featureless near-exponential decrease with increasing wavelength, moving from the ultraviolet to the visible region (Figure 1). In the non-irradiated sample, a shoulder is visible in the 250–290 nm region.

A gradual decrease in the absorption values was observed at increasing irradiation energy (Figure 1, Table 1). The $a_{254}$ and $a_{350}$ underwent a 3–22% and 25–54% reduction, respectively; the smaller effect was observed with Vis irradiation (3 and 25 % at 254 and 350 nm, respectively). The irradiation with the other cutoffs had the same effect on $a_{254}$ (19–22% reduction), whereas a slightly different effect was observed for $a_{350}$ (47 to 54% reduction) (Table 1). The 250–290 nm shoulder, which was observed in the non-irradiated samples, was gradually reduced with increasing irradiation energy and it was almost completely removed in the FS irradiated samples (Figure 1). The $SUVA_{254}$ underwent a 10–19% reduction with irradiation, with the higher effect being observed in the FS irradiated samples. The spectral slopes, both $S_{275–295}$, Sr, and the MS index increased with irradiation, with increasing effects at increasing irradiation energy. The Vis irradiation induced a 20% and 30% increase in the slopes and MS, respectively. The maximum increase (57–59% for the slopes and up to 74% for the MS) was observed with the FS irradiation (Table 1).

**Table 1.** Values of CDOM absorption indices before and after irradiation with different cutoff filters. Δ% indicates the difference between the irradiated sample and the non-irradiated one. The values refer to the average and standard deviation between the replicates.

| | DOC (μM) | | $a_{254}$ ($m^{-1}$) | | $a_{350}$ ($m^{-1}$) | | MS ($a_{250}/a_{365}$) | | $S_{275-295}$ ($nm^{-1}$) | | Sr | | $SUVA_{254}$ ($m^2\ g^{-1}$ C) | |
|---|---|---|---|---|---|---|---|---|---|---|---|---|---|---|
| | Average ± st. dev. | Δ% | Average ± st. dev. | Δ% | Average ± st. dev. | Δ% | Average ± st. dev. | Δ% | Average ± st. dev. | Δ% | Average ± st. dev. | Δ% | Average ± st. dev. | Δ% |
| Not Irr | 1190 ± 6 | | 44.8 ± 0.6 | | 6.8 ± 0.11 | | 9.8 ± 0.8 | | 0.0193 ± 0.0012 | | 0.883 ± 0.012 | | 1.37 ± 0.05 | |
| Vis | n.a. | n.a. | 43.3 ± 0.4 | **−3%** | 5.10 ± 0.05 | **−25%** | 12.6 ± 0.3 | **30%** | 0.0231 ± 0.0008 | **20%** | 1.062 ± 0.101 | **20%** | n.a. | n.a. |
| $I_{320-800}$ | 1066 ± 5 | **−10%** | 36.2 ± 0.5 | **−19%** | 3.60 ± 0.01 | **−47%** | 14.8 ± 0.6 | **52%** | 0.0278 ± 0.0006 | **44%** | 1.377 ± 0.095 | **56%** | 1.23 ± 0.02 | **−10%** |
| $I_{305-800}$ | 998 ± 2 | **−16%** | 35.1 ± 0.4 | **−22%** | 3.52 ± 0.10 | **−49%** | 14.9 ± 0.4 | **52%** | 0.0276 ± 0.0016 | **43%** | 1.325 ± 0.118 | **50%** | 1.28 ± 0.05 | **−7%** |
| $I_{295-800}$ | 1074 ± 6 | **−10%** | 34.6 ± 0.3 | **−22%** | 3.33 ± 0.32 | **−54%** | 15.5 ± 1.6 | **59%** | 0.0295 ± 0.0005 | **53%** | 1.416 ± 0.035 | **60%** | 1.17 ± 0.03 | **−14%** |
| FS | 1156 ± 4 | **−3%** | 35.2 ± 0.0 | **−21%** | 3.16 ± 0.02 | **−53%** | 17.0 ± 0.1 | **74%** | 0.0306 ± 0.0001 | **59%** | 1.388 ± 0.007 | **57%** | 1.10 ± 0.01 | **−19%** |

n.a.: data not available.

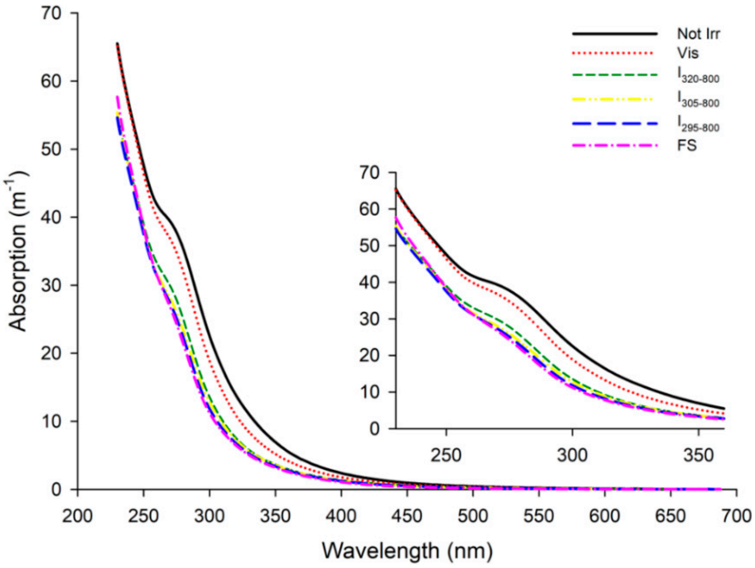


**Figure 1.** Absorption spectra of chromophoric dissolved organic matter (CDOM) released by E. huxleyi measured before and after the irradiation with the different cutoff filters. A zoom of the spectra between 230 and 400 nm is also shown, because this is the region where the major differences were observed. For each treatment the spectrum shown is the average spectra of the replicates.

### 3.3. Absorption Spectra of Degraded Molecules

The hypothetical absorption spectra of the compounds that were lost during irradiation were obtained by subtracting the spectra among themselves (Figure 2). In details:

- Spectrum of the compounds degraded by FS = spectrum of non-irradiated sample—spectrum of sample irradiated with FS.
- Spectrum of the compounds degraded by Vis = spectrum of non-irradiated sample—spectrum of sample irradiated with Vis (i.e., 395–800 nm).
- Spectrum of the compounds degraded by $I_{295–800}$ = spectrum of non-irradiated sample—spectrum of sample irradiated with $I_{295–800}$
- Spectrum of the compounds degraded by UV = spectrum a (degraded by FS)—spectrum b (degraded by Vis).

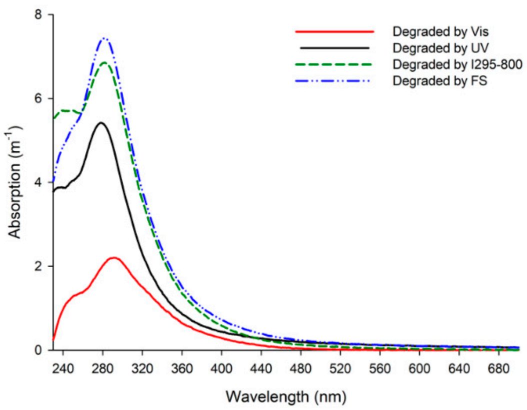


**Figure 2.** Hypothetical absorption spectra of compounds degraded by different irradiations. For each treatment the spectrum shown is the average spectra of the replicates.

The subtracted spectra showed well-resolved peaks and shoulders at different wavelengths. All of the spectra showed a major peak between 280 and 290 nm (Figure 2), which was higher in the sample that was degraded by FS and decreased at decreasing irradiation energy (Figure 2). Assuming that 100% of these chromophores were degraded by FS, then 92% was degraded by the $I_{295–800}$ irradiation, which suggested that the 280–295 radiation is responsible for only 8% of degradation, 70% was degraded by UV, and 30% by Vis radiation.

By applying the same calculation, the $I_{295–800}$ degraded 91% of $a_{350}$ and 100% of $a_{254}$, UV irradiation degraded 57% of $a_{350,}$ and 76% of $a_{254}$, and Vis irradiation degraded 43% of $a_{350}$ and 24% of $a_{254}$.

*3.4. CDOM Fluorescence*

The fluorescence emission spectra of the non-irradiated samples, excited at both 280 nm and 290 nm, showed a peak between 340 and 355 nm and a broad shoulder between 400 and 450 nm (Figure 3). The emission spectra of the non-irradiated samples excited at 355 nm showed only one peak at 435 nm. The emission spectra of the irradiated samples clearly showed a marked decrease in fluorescence and a slight shift in the fluorescence peaks. All of the spectra of the irradiated samples, excited both at 280 and 290 nm, showed a blue shift in the peaks of up to 11 nm with respect to the non-irradiated samples. The maximum effect of the irradiation was observed in the FS irradiated samples, excited at 290 nm, where the peak at 350 nm became less intense than the second shoulder (Figure 3). All of the emission spectra of the irradiated samples, which were excited at 355 nm, showed a red shift in the peak, with up to 9 nm difference with respect to the non-irradiated samples (Figure 3).

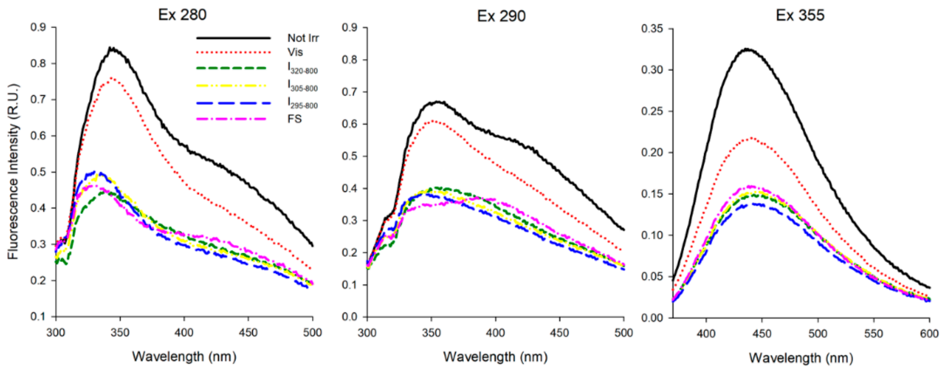


**Figure 3.** Fluorescence emission spectra at 280, 290 and 355 nm excitation wavelength (Ex 280, Ex 290, and Ex 355, respectively) of CDOM released by E. huxleyi before and after irradiation with the different cutoff filters. For each treatment the spectrum shown is the average spectra of the replicates. Note the difference in the scale of both axes.

In order to quantify the effect of irradiation on fluorescence, the area under each emission spectrum was calculated and the areas of the irradiated samples were compared with that of the non-irradiated samples. Among the three excitation wavelengths, the Vis irradiation showed the smallest effect, with a reduction of fluorescence of 13% at 280 nm excitation, 20% at 290 nm excitation, and 35% at 355 nm excitation, with respect to the non-irradiated samples. All the other irradiations caused > 50% decrease in fluorescence (Table 2).

**Table 2.** Values of CDOM fluorescence peaks and emission spectra area, before and after irradiation with different cutoff filters. Δ% indicates the difference between the irradiated sample and the non-irradiated one. The values refer to the average and standard deviation between the replicates.

| | **A (R.U.)** | | **C (R.U.)** | | **M (R.U.)** | | **T (R.U.)** | | **B (R.U.)** | | **$\lambda_{ex}$ 280 nm** | | **$\lambda_{ex}$ 290 nm** | | **$\lambda_{ex}$ 355 nm** | |
|---|---|---|---|---|---|---|---|---|---|---|---|---|---|---|---|---|
| | Average ± st. dev. | Δ% | Average ± st. dev. | Δ% | Average ± st. dev. | Δ% | Average ± st. dev. | Δ% | Average ± st. dev. | Δ% | Average ± st. dev. | Δ% | Average ± st. dev. | Δ% | Average ± st. dev. | Δ% |
| Not Irr | 0.656 ± 0.007 | | 0.429 ± 0.008 | | 0.660 ± 0.007 | | 0.871 ± 0.033 | | 0.384 ± 0.019 | | 62.60 ± 0.57 | | 68.63 ± 1.03 | | 20.53 ± 0.36 | |
| Vis | 0.566 ± 0.004 | **−14%** | 0.282 ± 0.009 | **−34%** | 0.508 ± 0.006 | **−23%** | 0.798 ± 0.029 | **−8%** | 0.360 ± 0.021 | **−6%** | 54.29 ± 1.02 | **−13%** | 55.16 ± 0.83 | **−20%** | 20.53 ± 0.68 | **−35%** |
| $I_{320\text{-}800}$ | 0.365 ± 0.002 | **−44%** | 0.184 ± 0.008 | **−57%** | 0.370 ± 0.012 | **−43%** | 0.502 ± 0.031 | **−42%** | 0.237 ± 0.019 | **−38%** | 28.20 ± 0.47 | **−55%** | 39.59 ± 0.18 | **−51%** | 13.41 ± 0.83 | **−57%** |
| $I_{305\text{-}800}$ | 0.356 ± 0.005 | **−45%** | 0.196 ± 0.003 | **−54%** | 0.362 ± 0.002 | **−45%** | 0.486 ± 0.032 | **−44%** | 0.236 ± 0.017 | **−39%** | 27.06 ± 1.33 | **−57%** | 31.40 ± 0.54 | **−54%** | 14.07 ± 0.22 | **−55%** |
| $I_{295\text{-}800}$ | 0.343 ± 0.009 | **−47%** | 0.181 ± 0.010 | **−58%** | 0.340 ± 0.009 | **−48%** | 0.477 ± 0.023 | **−45%** | 0.238 ± 0.018 | **−38%** | 27.10 ± 1.12 | **−57%** | 29.11 ± 0.79 | **−58%** | 13.29 ± 0.59 | **−58%** |
| FS | 0.412 ± 0.004 | **−37%** | 0.208 ± 0.001 | **−52%** | 0.442 ± 0.008 | **−33%** | 0.442 ± 0.035 | **−49%** | 0.220 ± 0.023 | **−43%** | 26.47 ± 2.97 | **−58%** | 32.50 ± 0.80 | **−53%** | 15.21 ± 0.04 | **−52%** |

### *3.5. Fluorescence Spectra of Molecules Degraded by Irradiation*

The hypothetical fluorescence emission spectra of the compounds that were degraded by irradiation were obtained by subtracting the spectra among themselves in the same way as it was done for the absorption spectra (see Section 3.3).

The subtracted spectra showed well-resolved peaks and shoulders at different wavelengths. In the spectra, which were excited at both 280 and 290 nm, photodegradation removed compounds with an emission peak at approximately 350 nm (Figure 4). In the spectra excited at 290, nm the removal of the compounds emitting at ≈ 430 nm is more accentuated than in the spectra that were excited at 280 nm.

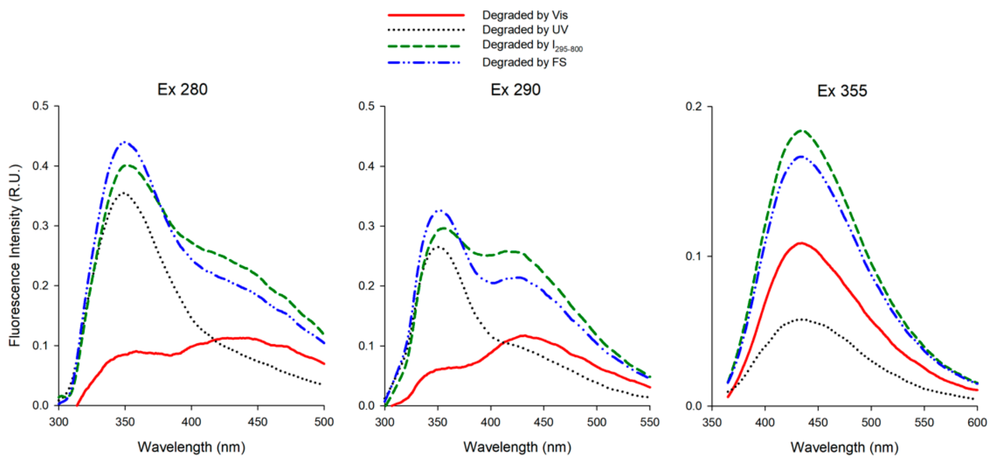


**Figure 4.** Hypothetical emission spectra of the compounds that were degraded by irradiation. For each treatment the spectrum shown is the average spectra of the replicates. Note the difference in the scale of both axes.

In the spectra, excited at 355 nm, the only compounds removed were those with an emission peak at ≈ 430 nm. It is noteworthy that the UV removed less fluorescence than the Vis irradiation.

### *3.6. CDOM EEMs*

In order to investigate the changes in CDOM fluorescence peak, picking was chosen instead of parallel factor analysis (PARAFAC because of the limited number of samples measured (i.e., 12). The typical CDOM fluorophores peaks [43] were identified on the EEMs and their changes in intensity were evaluated after irradiation (Figure 5, Table 2).

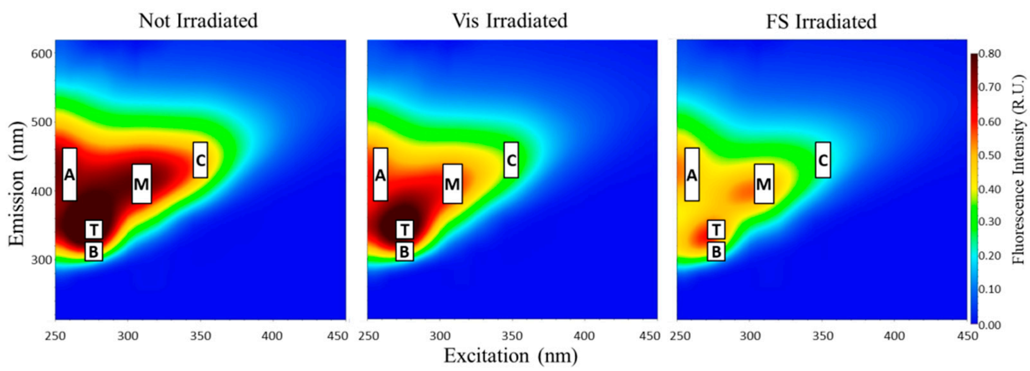


**Figure 5.** Examples of Excitation-Emission matrixes (EEMs) of CDOM released by *E. huxleyi* measured before and after irradiation with Vis and FS. The typical CDOM fluorophores are shown on the EEMs.

In the non-irradiated samples, all the peaks are well visible and the protein-like peak T is the most intense, followed by the humic-like peaks (A, M, and C), and the tyrosine-like peak B is the least fluorescent (Figure 5, Table 2). All of the irradiation wavelengths caused a significant decrease in the fluorescence of all the peaks (Figure 5, Table 2). The Vis irradiation was the one with the lowest effect, causing only a 6–8% decrease in the protein-like peaks B and T, respectively, and a 14 to 34% decrease in the humic-like peaks. Peak C was the most affected by all of the irradiation wavelengths, showing a reduction of intensity up to 58% with $I_{295–800}$. Overall the humic-like peaks were the most affected by irradiation, except for the FS irradiation. With FS irradiation, the protein-like peaks T and B (−49 and −43%) were more degraded than peaks A and M (−37 and −33%).

Looking more in detail at the percentage of reduction of each peak, it is possible to notice that the effect of irradiation on the protein-like peaks T and B increases with increasing irradiation energy, and that $I_{295–800}$ $I_{305–800}$, and $I_{320–800}$ had similar effects. The humic-like peaks (A, C, and M) instead do not show this correlation with irradiation energy, with FS irradiation having a lower effect than $I_{295–800}$ $I_{305–800}$, and $I_{320–800}$ (Table 2).

## 4. Discussion

### 4.1. DOM Photomineralization

The results of this experiment show that the irradiation of DOM, released by *E. huxleyi*, induced the removal of 10–16% of DOC. These results are similar to those that were reported by Bittar et al. [24]. These authors showed that the photomineralization of algal DOM removed 19% of DOC after 1 week of irradiation. The shorter time (10 h) of our experiment needed to reach the same percentage of photomineralization may be attributed to the different irradiation wavelengths that were used in our experiment, Bittar et al. [24] used only UV-B light (275–315 nm). At the same time, the almost absence of photomineralization in the FS irradiated samples (3%) is in agreement with the results of Blanchet et al. [22]. These authors observed no decrease in algal DOC concentration with an irradiation similar to our FS (280–700 nm). Additionally, similar results were shown by Thomas and Lara [44]. These authors observed a change in DOC concentration of 10–15% after photodegradation of algal DOM, which was not significantly different from the control samples.

The difference in photomineralization between the cutoffs and the FS was unexpected. To the best of our knowledge, there is only another study where irradiation with different cutoffs was applied and DOC concentration was measured. Osburn et al. [3] used several cutoffs between 305 and 395 nm and their results showed an increase in photomineralization with increasing irradiation energy. However, it is difficult to compare the results, because these authors used riverine DOM for their experiments, and it has been already shown that photochemical processes differently affected algal and riverine DOM.

Overall, our results suggest a photomineralization effect on algal DOM, which is smaller than that previously reported for terrestrial DOM, being up to 30% [3,21].

### 4.2. DOM Photobleaching

#### 4.2.1. Absorption Spectra

The value of $a_{254}$ in the non-irradiated samples, i.e., in the algal exudates, is substantially higher than those that were reported for the open seawater [34,45,46]. This is not surprising, and it is probably due to the much higher CDOM concentration in algal exudates than in seawater. Probably, due to the high concentration, the shoulder at 250–290 nm was also visible. This shoulder is typical of algal DOM [47,48] and can be attributed to the presence of a great amount of low molecular weight poly-unsaturated and aromatic compounds [9]. After irradiation, a significant decrease in the absorption was observed, which suggested the photodegradation of a large amount of CDOM. These results are similar to those that were reported by Blanchet et al. [22], who observed up to 71% decrease of $a_{350}$ after irradiation of algal DOM. The smaller percentage of removal observed in our experiment (up to 54% of $a_{350}$) might be attributed to the shorter irradiation time (10 h vs. 24 h).

The maximum removal of absorption was observed at 280–290 nm, as shown from the well-resolved peak in the subtracted spectra (Figure 2), which indicates that the photodegradation mainly affects the low molecular weight poly-unsaturated and aromatic compounds released by phytoplankton. The shoulder at 250–290 nm was markedly reduced by irradiation (Figure 1).

The values of $S_{275–295}$ of the non-irradiated samples (Table 1) were lower than those reported for open seawater (0.02–0.047 $nm^{-1}$; [34,45,46]). These values indicate that the molecules present in CDOM released by *E. huxleyi* are on average bigger and with a higher aromatic content than CDOM in open sea waters. This is consistent with the release of these molecules by *E. huxleyi*, which have not undergone any transformation. As expected, the irradiation caused a marked increase of all the absorption indices (i.e., $S_{275–295}$, Sr, and MS) and a decrease in $SUVA_{254}$, suggesting a decrease in molecular weight and aromaticity of the molecules. These results are in agreement with previous findings on both algal and terrestrial DOM [16,18,25,35].

#### 4.2.2. Irradiation Affects Differently Humic-Like and Protein-Like Substances

The fluorescence spectra and the EEMs both showed the presence of protein-like and humic-like compounds. In the fluorescence spectra excited at 280/290 nm, the emission peak at 340/355 nm is attributed to the fluorescence of protein-like compounds, whereas the shoulder at 400–450 nm is due to the presence of humic-like compounds [38,39]. In the emission spectra that were excited at 355 nm, only one peak, attributed to the humic-like substances, is visible (Figure 3). It is noteworthy that the protein-like peaks are dominant. This is consistent with recently produced algal DOM [49], whereas, in seawater, the protein-like fluorescence is usually much diluted and, consequently, difficult to detect.

In the EEMs of the non-irradiated samples peak T, attributed to tryptophan-like compounds, was the dominant peak followed by peak M, whereas the tyrosine-like peak (peak B) was the less intense. These results are in good agreement with those reported by Romera-Castillo et al. [49]. These authors observed the production of both protein-like and humic-like substances by marine phytoplankton and showed that peaks T and M were the main peaks in CDOM released by different species of phytoplankton.

The effect of irradiation was different on the protein-like and humic-like fluorescence and changed according to the cutoff filters used. The effect on the protein-like fluorescence was proportional to the energy of the irradiation (Figures 3 and 4, Table 2).

A difference between the spectra excited at 280 and 290 nm should also be noted. In the latter, the 350 nm peak loses its "peak shape" when irradiated with FS. With this excitation wavelength being selective for tryptophan residues [40], this finding suggests that the tryptophan present in the algal CDOM was more sensible to photobleaching by FS irradiation than the other aromatic amino acids. Surprisingly, the photodegradation of humic-like fluorescence did not directly correlate with the irradiation energy. The Vis irradiation had a higher photodegradation effect on humic-like substances than UV irradiation and the FS irradiation had less effect than the $I_{295–800}$ (Figure 4). The same pattern can be observed in the 400–450 nm emission range in the spectra excited at 280 and 290 nm, where the effect of the different irradiation wavelengths on proteins is also evident (Figure 4). The lower effect of FS irradiation as compared to $I_{295–800}$, $I_{305–800}$, and $I_{320–800}$ is also well shown by the variation in the EEMs peaks A, C, and M (Table 2). This observation is not easy to explain, since FS is inclusive of all the other wavelengths, including those with the highest energy (<295 nm). How can it have less effect on humic-like substances than $I_{295–800}$? One possibility is that the FS irradiation might change the quantum yield of these fluorophores, resulting in an increase of fluorescence, even if the fluorophores are less than in the non-irradiated sample. The higher energetic irradiation <295 nm in the FS irradiation might induce a conformational modification in the chromophores, resulting in a changed quantum yield.

In general, the irradiation had a higher effect on humic substances than on proteins, as also known from previous studies [50]. Taking into consideration all of the irradiation wavelengths, the humic-like peaks (C, M, and A) are the most photodegraded. However, FS irradiation is an exception to this behavior since peaks A and M were less affected than peaks B and T. The higher effect of FS irradiation on the protein-like peaks (T and B) might be attributed to the presence, in the proteins of more high energy bonds than in the humic acids; these bonds can only be broken by wavelengths < 295 nm, only present in the FS. The higher energy UV irradiation, present in the FS, can lead to the production of radical species, such as OH radicals [51], which can break the high energy bonds in proteins. However, this is only a possibility, and these behaviors need to be examined more in-depth with further experiments.

### 4.3. Implications

Recent models showed that we should, expect in the near future, an increase in solar radiation in some regions of the globe, e.g., in the northern Mediterranean area [52–54]. It is also important to consider that the expected increased stratification of the upper layers of the Mediterranean Sea due to global warming, should induce an increase in the dose of UV and visible radiation that is received by planktonic organisms [55]. If we reflect our results in the context of these anticipated effects of climate change on irradiation, some considerations can be made. Our results showed that algal DOM undergoes mostly photobleaching, rather than photomineralization, after light exposure. Therefore, an increased irradiation might lead to an increased photobleaching of algal DOM. The effect of the increased photobleaching can be twofold. On one side, there will be a higher amount of DOM transformed into more bioavailable, smaller compounds that stimulate the microbial-loop with cascade effects on higher trophic levels ([2] and references therein). On the other side, since CDOM in the oceans dominates the absorption in the blue and visible range of the spectra, a reduction of CDOM absorption in the surface will allow for a deeper penetration of the radiation in the water column, including harmful UV radiations, which can damage plankton populations [2], resulting in a reduced primary production. This process could, in turn, lead to a reduced production of autochthonous algal DOM.

The consequences of a higher irradiation and increased DOM photobleaching are not easy to predict; for this reason, the results of this study, and similar ones, should be taken into account in predictive models, to attempt having more precise insights of what these effects might be.

Additionally, our results confirmed that algal DOM undergoes less photomineralization with respect to terrestrial DOM. Because oceanic DOM is mostly constituted by freshly produced autochthonous algal DOM, this difference in photomineralization rates points out to the need of a deeper investigation on algal DOM photodegradation in order to have better estimates of DOC loss from algal DOM photomineralization. These estimates are fundamental to be taken into account when making oceanic carbon budgets, since the extrapolation of DOC removal rates and $CO_2$ release to the atmosphere, obtained from terrestrial DOM photodegradation experiments, which are the majority, might not be appropriate.

## 5. Summary and Conclusions

The results of our study showed that algal DOM that is produced by *Emiliania huxleyi* is highly affected by photobleaching. A small photomineralization was observed, with a loss of 10–16% of DOC. The efficiency of photobleaching on absorption parameters was strictly dependent on the energy of irradiation. Indeed, the highest loss in CDOM absorption was observed with the full sun spectrum irradiation (i.e., 280–800 nm) and the lowest one with the visible irradiation (i.e., 395–800 nm). The absorption indices (i.e., MS, $S_{275–295}$, Sr, and $SUVA_{254}$) point out changes in the properties of the molecules, becoming smaller and less aromatic after irradiation. Our data further support that these indices can be a good tracer of the photochemical history of CDOM. The effect of photobleaching on fluorescence was different for protein-like and humic-like substances. The protein-like fluorescence decreased gradually with increasing irradiation energy, similarly to the absorption, showing a maximum bleaching of 49%. Instead, the humic-like fluorescence did not show a linear trend between photobleaching and irradiation energy, suggesting a change in these molecules' quantum yield.

**Author Contributions:** Conceptualization, C.S., B.C., and R.S.; methodology, S.V., F.V., B.C., C.S.; formal analysis, S.V., C.S., M.G., B.C., S.R.B.; investigation, C.S., M.G., B.C., S.R.B.; data curation, S.R.B.; writing—original draft preparation, M.G., S.R.B.; writing—review and editing, S.R.B., B.C., M.G., F.V., R.S., S.V., C.S.; funding acquisition, C.S., B.C., R.S. All authors have read and agreed to the published version of the manuscript.

**Funding:** This research was funded by thanks to the CHP Galileo, implemented by the Ministry of Europe and Foreign Affairs (MEAE) and the Ministry of Higher Education, Research and Innovation (MESRI) and in the partner country by the Ministero dell'Istruzione, dell' Università e della Ricerca (MIUR). This work was carried out in the framework of the bilateral scientific cooperation agreement between CNR and CNRS 2012–2013, project title "Impact of CDOM chemical composition on light availability in Mediterranean Ecosystem".

**Conflicts of Interest:** The authors declare no conflict of interest. The funders had no role in the design of the study; in the collection, analyses, or interpretation of data; in the writing of the manuscript, or in the decision to publish the results.

## References

1. Carlson:, C.A.; Hansell, D.A. DOM Sources, Sinks, Reactivty, and Budgets. In *Biogeochemistry of Marine Dissolved Organic Matter*; Academic Press: Cambridge, UK, 2015; pp. 65–126. ISBN 9780124059405.
2. Mopper, K.; Kieber, D.J.; Stubbins, A. Marine Photochemistry of Organic Matter: Processes and Impacts. Processes and Impacts. In *Biogeochemistry of Marine Dissolved Organic Matter*, 2nd ed.; Academic Press: Cambridge, UK, 2015; ISBN 9780124059405.
3. Osburn, C.L.; Retamal, L.; Vincent, W.F. Photoreactivity of chromophoric dissolved organic matter transported by the Mackenzie River to the Beaufort Sea. *Mar. Chem.* **2009**, *115*, 10–20. [CrossRef]
4. Lindell, M.J.; Granéli, H.W.; Bertilsson, S. Seasonal photoreactivity of dissolved organic matter from lakes with contrasting humic content. *Can. J. Fish. Aquat. Sci.* **2000**, *57*, 875–885. [CrossRef]
5. Tedetti, M.; Kawamura, K.; Narukawa, M.; Joux, F.; Charrière, B.; Sempéré, R. Hydroxyl radical-induced photochemical formation of dicarboxylic acids from unsaturated fatty acid (oleic acid) in aqueous solution. *J. Photochem. Photobiol. A Chem.* **2007**, *188*, 135–139. [CrossRef]
6. Gonsior, M.; Peake, B.M.; Cooper, W.T.; Podgorski, D.; D'Andrilli, J.; Cooper, W.J. Photochemically induced changes in dissolved organic matter identified by ultrahigh resolution fourier transform ion cyclotron resonance mass spectrometry. *Environ. Sci. Technol.* **2009**, *43*, 698–703. [CrossRef] [PubMed]
7. Ward, C.P.; Cory, R.M. Complete and Partial Photo-oxidation of Dissolved Organic Matter Draining Permafrost Soils. *Environ. Sci. Technol.* **2016**, *50*, 3545–3553. [CrossRef] [PubMed]
8. Ortega-Retuerta, E.; Pulido-Villena, E.; Reche, I. Effects of dissolved organic matter photoproducts and mineral nutrient supply on bacterial growth in Mediterranean inland waters. *Microb. Ecol.* **2007**, *54*, 161–169. [CrossRef]
9. Swan, C.M.; Nelson, N.B.; Siegel, D.A.; Kostadinov, T.S. The effect of surface irradiance on the absorption spectrum of chromophoric dissolved organic matter in the global ocean. *Deep. Res. Part I Oceanogr. Res. Pap.* **2012**, *63*, 52–64. [CrossRef]
10. Núñez-Pons, L.; Avila, C.; Romano, G.; Verde, C.; Giordano, D. UV-protective compounds in marine organisms from the southern ocean. *Mar. Drugs* **2018**, *16*, 336. [CrossRef] [PubMed]
11. Moran, M.; Zepp, R. Role of photoreactions in the formation of biologically labile compounds from dissolved organic matter. *Limnol. Oceanogr.* **1997**, *42*, 1307–1316. [CrossRef]
12. Obernosterer, I.; Reitner, B.; Herndl, G.J. Contrasting effects of solar radiation on dissolved organic matter and its bioavailability to marine bacterioplankton. *Limnol. Oceanogr.* **1999**, *44*, 1645–1654. [CrossRef]
13. Tranvik, L.J.; Bertilsson, S. Contrasting effects of solar UV radiation on dissolved organic sources for bacterial growth. *Ecol. Lett.* **2001**, *4*, 458–463. [CrossRef]
14. Mopper, K.; Kieber, D.J. Photochemistry and the Cycling of Carbon, Sulfur, Nitrogen and Phosphorus. In *Biogeochemistry of Marine Dissolved Organic Matter*; Academic Press: Cambridge, UK, 2002.
15. Zepp, R.G.; Erickson, D.J.; Paul, N.D.; Sulzberger, B. Effects of solar UV radiation and climate change on biogeochemical cycling: Interactions and feedbacks. *Photochem. Photobiol. Sci.* **2011**, *10*, 261–279. [CrossRef] [PubMed]
16. Osburn, C.L.; O'Sullivan, D.W.; Boyd, T.J. Increases in the longwave photobleaching of chromophoric dissolved organic matter in coastal waters. *Limnol. Oceanogr.* **2009**, *54*, 145–159. [CrossRef]

17. Timko, S.A.; Maydanov, A.; Pittelli, S.L.; Conte, M.H.; Cooper, W.J.; Koch, B.P.; Schmitt-Kopplin, P.; Gonsior, M. Depth-dependent photodegradation of marine dissolved organic matter. *Front. Mar. Sci.* **2015**, *2*, 66. [CrossRef]
18. Zagarese, H.E.; Diaz, M.; Pedrozo, F.; Ferraro, M.; Cravero, W.; Tartarotti, B. Photodegradation of natural organic matter exposed to fluctuating levels of solar radiation. *J. Photochem. Photobiol. B Biol.* **2001**, *61*, 35–45. [CrossRef]
19. Para, J.; Coble, P.G.; Charrière, B.; Tedetti, M.; Fontana, C.; Sempéré, R. Fluorescence and absorption properties of chromophoric dissolved organic matter (CDOM) in coastal surface waters of the northwestern Mediterranean Sea, influence of the Rhône River. *Biogeosciences* **2010**, *7*, 4083–4103. [CrossRef]
20. Tedetti, M.; Joux, F.; Charrière, B.; Mopper, K.; Sempéré, R. Contrasting effects of solar radiation and nitrates on the bioavailability of dissolved organic matter to marine bacteria. *J. Photochem. Photobiol. A Chem.* **2009**, *201*, 243–247. [CrossRef]
21. Moran, M.A.; Sheldon, W.M.; Zepp, R.G. Carbon loss and optical property changes during long-term photochemical and biological degradation of estuarine dissolved organic matter. *Limnol. Oceanogr.* **2000**, *45*, 1254–1264. [CrossRef]
22. Blanchet, M.; Fernandez, C.; Joux, F. Photoreactivity of riverine and phytoplanktonic dissolved organic matter and its effects on the dynamics of a bacterial community from the coastal Mediterranean Sea. *Prog. Oceanogr.* **2018**, *163*, 82–93. [CrossRef]
23. Osburn, C.L.; Zagarese, H.E.; Morris, D.P.; Hargreaves, B.R.; Cravero, W.E. Calculation of spectral weighting functions for the solar photobleaching of chromophoric dissolved organic matter in temperate lakes. *Limnol. Oceanogr.* **2001**, *46*, 1455–1467. [CrossRef]
24. Bittar, T.B.; Stubbins, A.; Vieira, A.A.H.; Mopper, K. Characterization and photodegradation of dissolved organic matter (DOM) from a tropical lake and its dominant primary producer, the cyanobacteria Microcystis aeruginosa. *Mar. Chem.* **2015**, *177*, 205–217. [CrossRef]
25. Liu, S.; Feng, W.; Song, F.; Li, T.; Guo, W.; Wang, B.B.; Wang, H.; Wu, F. Photodegradation of algae and macrophyte-derived dissolved organic matter: A multi-method assessment of DOM transformation. *Limnologica* **2019**, *77*, 125683. [CrossRef]
26. Winter, A.; Henderiks, J.; Beaufort, L.; Rickaby, R.E.M.; Brown, C.W. Poleward expansion of the coccolithophore Emiliania huxleyi. *J. Plankton Res.* **2014**, *36*, 316–325. [CrossRef]
27. Winter, A.; Siesser, W.G. *Coccolithophores*; Cambridge University Press: Cambridge, UK, 2006.
28. Balch, W.M. The ecology, biogeochemistry, and optical properties of coccolithophores. *Ann. Rev. Mar. Sci.* **2018**, *10*, 71–98. [CrossRef]
29. Jeffrey, S.W.; LeRoi, J.-M. Simple procedures for growing SCOR reference microalgal cultures. In *Phytoplankton Pigments in Oceanography: Monographs on Oceanographic Methodology*; UNESCO: Paris, France, 1997; ISBN 9789231032752.
30. Fichot, C.G.; Benner, R. A novel method to estimate DOC concentrations from CDOM absorption coefficients in coastal waters. *Geophys. Res. Lett.* **2011**, *38*, 1–5. [CrossRef]
31. Santinelli, C.; Follett, C.; Retelletti Brogi, S.; Xu, L.; Repeta, D. Carbon isotope measurements reveal unexpected cycling of dissolved organic matter in the deep Mediterranean Sea. *Mar. Chem.* **2015**, *177*, 267–277. [CrossRef]
32. Hansell, D.A. Dissolved Organic Carbon Reference Material Program. *Eos. Trans. Am. Geophys. Union* **2005**, *86*, 318. [CrossRef]
33. Omanović, D.; Santinelli, C.; Marcinek, S.; Gonnelli, M. ASFit—An all-inclusive tool for analysis of UV–Vis spectra of colored dissolved organic matter (CDOM). *Comput. Geosci.* **2019**, *133*, 104334. [CrossRef]
34. Iuculano, F.; Álvarez-Salgado, X.A.; Otero, J.; Catalá, T.S.; Sobrino, C.; Duarte, C.M.; Agustí, S. Patterns and drivers of UV absorbing chromophoric dissolved organic matter in the euphotic layer of the open ocean. *Front. Mar. Sci.* **2019**, *6*, 320. [CrossRef]
35. Helms, J.R.; Stubbins, A.; Ritchie, J.D.; Minor, E.C.; Kieber, D.J.; Mopper, K. Absorption spectral slopes and slope ratios as indicators of molecular weight, source, and photobleaching of chromophoric dissolved organic matter. *Limnol. Oceanogr.* **2008**, *53*, 955–969. [CrossRef]
36. Peuravuori, J.; Pihlaja, K. Molecular size distribution and spectroscopic properties of aquatic humic substances. *Anal. Chim. Acta* **1997**, *337*, 133–149. [CrossRef]

37. Weishaar, J.; Aiken, G.; Bergamaschi, B.; Fram, M.; Fujii, R.; Mopper, K. Evaluation of specific ultra-violet absorbance as an indicator of the chemical content of dissolved organic carbon. *Environ. Sci. Technol.* **2003**, *37*, 4702–4708. [CrossRef] [PubMed]
38. Seritti, A.; Russo, D.; Nannicini, L.; Del Vecchio, R. DOC, absorption and fluorescence properties of estuarine and coastal waters of the Northern Tyrrhenian Sea. *Chem. Speciat. Bioavailab.* **1998**, *10*, 95–106. [CrossRef]
39. Vignudelli, S.; Santinelli, C.; Murru, E. Distributions of dissolved organic carbon (DOC) and chromophoric dissolved organic matter (CDOM) in coastal waters of the northern Tyrrhenian Sea (Italy). *Estuar. Coast. Shelf Sci.* **2004**, *60*, 133–149. [CrossRef]
40. Lakowicz, J.R. *Principles of Fluorescence Spectroscopy*; Springer: Berlin/Heidelberg, Germany, 2006; ISBN 0387312781.
41. Lawaetz, A.J.; Stedmon, C.A. Fluorescence intensity calibration using the Raman scatter peak of water. *Appl. Spectrosc.* **2009**, *63*, 936–940. [CrossRef] [PubMed]
42. Carlson, R.E.; Fritsch, F.N. An Algorithm for Monotone Piecewise Bicubic Interpolation. *SIAM J. Numer. Anal.* **1989**, *26*, 230–238. [CrossRef]
43. Coble, P.G. Marine optical biogeochemistry: The chemistry of ocean color. *Chem. Rev.* **2007**, *107*, 402–418. [CrossRef]
44. Thomas, D.N.; Lara, R.J. Photodegradation of algal derived dissolved organic carbon. *Mar. Ecol. Prog. Ser.* **1995**, *116*, 309–310. [CrossRef]
45. Catalá, T.S.; Martínez-Pérez, A.M.; Nieto-Cid, M.; Álvarez, M.; Otero, J.; Emelianov, M.; Reche, I.; Arístegui, J.; Álvarez-Salgado, X.A. Dissolved Organic Matter (DOM) in the open Mediterranean Sea. I. Basin–wide distribution and drivers of chromophoric DOM. *Prog. Oceanogr.* **2018**, *165*, 35–51. [CrossRef]
46. Galletti, Y.; Gonnelli, M.; Retelletti Brogi, S.; Vestri, S.; Santinelli, C. DOM dynamics in open waters of the Mediterranean Sea: New insights from optical properties. *Deep. Res. Part I Oceanogr. Res. Pap.* **2019**, *144*, 95–114. [CrossRef]
47. Granskog, M.A.; Nomura, D.; Müller, S.; Krell, A.; Toyota, T.; Hattorl, H. Evidence for significant protein-like dissolved organic matter accumulation in Sea of Okhotsk sea ice. *Ann. Glaciol.* **2015**, *56*, 1–8. [CrossRef]
48. Wozniak, B.; Dera, J. *Light Absorption in Sea Water*; Springer: New York, NY, USA, 2007; Volume 33, ISBN1 0387307532. ISBN2 9780387307534.
49. Romera-Castillo, C.; Sarmento, H.; Alvarez-Salgado, X.A.; Gasol, J.M.; Marrase, C. Production of chromophoric dissolved organic matter by marine phytoplankton. *Limnol. Oceanogr.* **2010**, *55*, 446–454. [CrossRef]
50. Osburn, C.L.; Del Vecchio, R.; Boyd, T.J. Physicochemical Effects on Dissolved Organic Matter Fluorescence in Natural Waters. In *Aquatic Organic Matter Fluorescence*; Cambridge University Press: Cambridge, UK, 2014.
51. Mopper, K.; Zhou, X. Hydroxyl radical photoproduction in the sea and its potential impact on marine processes. *Science* **1990**, *250*, 661–664. [CrossRef] [PubMed]
52. Trenberth, K.E.; Fasullo, J.T. Global warming due to increasing absorbed solar radiation. *Geophys. Res. Lett.* **2009**, *36*. [CrossRef]
53. Gil, V.; Gaertner, M.A.; Gutierrez, C.; Losada, T. Impact of climate change on solar irradiation and variability over the Iberian Peninsula using regional climate models. *Int. J. Climatol.* **2019**, *39*, 1733–1747. [CrossRef]
54. Huber, I.; Bugliaro, L.; Ponater, M.; Garny, H.; Emde, C.; Mayer, B. Do climate models project changes in solar resources? *Sol. Energy* **2016**, *39*, 1733–1747. [CrossRef]
55. Sempéré, R.; Para, J.; Tedetti, M.; Charrière, B.; Mallet, M. Variability of Solar Radiation and CDOM in Surface Coastal Waters of the Northwestern Mediterranean Sea. *Photochem. Photobiol.* **2015**, *91*, 851–861. [CrossRef] [PubMed]